Lagrangian Formulation of a Spring Pendulum with Oscillating Magnetic Interaction

Contents

1 System Description **2**
- 1.1 Generalized Coordinates . . . 2
- 1.2 Kinetic Energy . . . 2
- 1.3 Potential Energy . . . 3
- 1.4 Lagrangian . . . 3

2 Equations of Motion **4**
- 2.1 Radial Motion (r) . . . 4
- 2.2 Angular Motion (θ) . . . 4

3 Numerical Methodology for the Spring Pendulum with Magnetic Interaction **4**

4 Numerical Schemes Considered **4**
- 4.1 Euler Method . . . 4
- 4.2 Verlet Integration . . . 5
- 4.3 Runge-Kutta Methods (RK4 and RK45) . . . 5
- 4.4 Implicit Backward Euler Method . . . 5
- 4.5 Crank-Nicolson Method . . . 5
- 4.6 Leapfrog Method . . . 5
- 4.7 Symplectic Integrators . . . 6
- 4.8 Exponential Integrators . . . 6
- 4.9 Multiscale Methods . . . 6
- 4.10 Geometric Integrators . . . 6
- 4.11 Methodology Selection . . . 6

5 Numerical Results and Visualizations **7**
- 5.1 Animation of the System Dynamics . . . 7
- 5.2 Radial Phase Portrait . . . 7
- 5.3 Angular Phase Portrait . . . 8
- 5.4 Poincaré Map . . . 8
- 5.5 Discussion of Results . . . 8

6 Magnetic Interaction Modeling **10**
6.1 Enhanced Magnetic Field Model 10
6.2 Nonlinear Magnetic Force 10
6.3 Updated Equations of Motion 10
6.4 Numerical Implementation 11
6.5 Discussion 11

7 Spring Pendulum with Magnetic Interaction: Numerical Analysis **11**

8 Numerical Techniques **11**

9 Enhanced Magnetics **11**
9.1 Radial Phase Portrait 12
9.2 Angular Phase Portrait 12
9.3 Poincaré Map 12
9.4 Animation 12

10 Discussion **13**

11 Conclusion **13**

1 System Description

We consider a spring pendulum system where:

- A mass m is attached to a spring with a spring constant k and natural length l_0.
- The mass is free to move in both radial (r) and angular (θ) directions.
- The mass is ferromagnetic with a magnetic moment μ, and is influenced by an oscillating magnetic field $B(t)$.
- The system is also subject to gravity, with gravitational acceleration g.

1.1 Generalized Coordinates

The system is described by the following coordinates:

- $r(t)$: The length of the spring.
- $\theta(t)$: The angular displacement of the pendulum from the vertical.

1.2 Kinetic Energy

The velocity of the mass can be expressed as:

$$v^2 = \dot{r}^2 + r^2\dot{\theta}^2$$

Thus, the kinetic energy is:

$$T = \frac{1}{2}m\left(\dot{r}^2 + r^2\dot{\theta}^2\right)$$

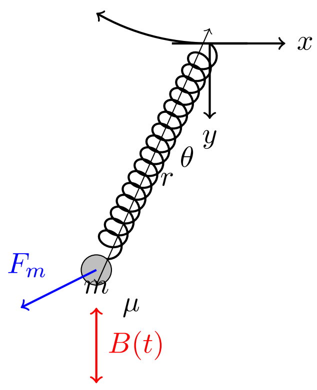

Figure 1: A diagram of the spring pendulum system with a ferromagnetic mass influenced by an oscillating magnetic field. The mass m is attached to the end of the spring, which extends from the fixed support. The system is free to move in both the radial (r) and angular (θ) directions. The mass has a magnetic moment μ, which interacts with the oscillating magnetic field $B(t)$, depicted by a red arrow. The blue arrow represents the magnetic force F_m, which affects the angular motion. The diagram also shows the coordinate system (x, y) and generalized coordinates r and θ.

1.3 Potential Energy

The potential energy includes:

1. **Gravitational Potential:**
$$U_g = -mgr\cos\theta$$
2. **Spring Potential:**
$$U_s = \frac{1}{2}k(r-l_0)^2$$
3. **Magnetic Interaction:** Assuming the magnetic field oscillates as $B(t) = B_0\cos(\omega t)$, the magnetic potential energy is:
$$U_m = -\mu B(t)\cos\theta = -\mu B_0\cos(\omega t)\cos\theta$$

The total potential energy is:

$$U = -mgr\cos\theta + \frac{1}{2}k(r-l_0)^2 - \mu B_0\cos(\omega t)\cos\theta$$

1.4 Lagrangian

The Lagrangian is defined as:

$$\mathcal{L} = T - U$$

Substituting the expressions for T and U:

$$\mathcal{L} = \frac{1}{2}m\left(\dot{r}^2 + r^2\dot{\theta}^2\right) + mgr\cos\theta - \frac{1}{2}k(r-l_0)^2 + \mu B_0\cos(\omega t)\cos\theta$$

2 Equations of Motion

The equations of motion are derived using the Euler-Lagrange equations:

$$\frac{d}{dt}\left(\frac{\partial \mathcal{L}}{\partial \dot{q}_i}\right) - \frac{\partial \mathcal{L}}{\partial q_i} = 0$$

where q_i are the generalized coordinates.

2.1 Radial Motion (r)

$$m\ddot{r} - mr\dot{\theta}^2 + k(r - l_0) - mg\cos\theta = 0$$

2.2 Angular Motion (θ)

$$\frac{d}{dt}\left(mr^2\dot{\theta}\right) + mgr\sin\theta - \mu B_0\cos(\omega t)\sin\theta = 0$$

3 Numerical Methodology for the Spring Pendulum with Magnetic Interaction

This section provides an overview of numerical methods for solving the coupled differential equations derived from the Lagrangian formulation of the spring pendulum system. The equations of motion for the radial (r) and angular (θ) directions involve time-dependent terms, nonlinear coupling, and periodic forcing due to the oscillating magnetic field. Thus, robust numerical schemes are essential to ensure stability, accuracy, and computational efficiency.

4 Numerical Schemes Considered

4.1 Euler Method

The Euler method is a straightforward first-order numerical scheme. Given an ordinary differential equation (ODE) of the form:

$$\frac{dy}{dt} = f(t, y),$$

the Euler method approximates the solution as:

$$y_{n+1} = y_n + hf(t_n, y_n),$$

where h is the time step size. While simple to implement, the Euler method is conditionally stable and can accumulate significant numerical error, especially for stiff or oscillatory systems [?].

4.2 Verlet Integration

Verlet integration is widely used for conservative systems. It approximates the position and velocity using:

$$r_{n+1} = 2r_n - r_{n-1} + h^2 a_n,$$

where a_n is the acceleration at time step n. This method is second-order accurate, time-reversible, and conserves energy over long simulations. However, it is less efficient when velocity-dependent terms are present [?].

4.3 Runge-Kutta Methods (RK4 and RK45)

The fourth-order Runge-Kutta (RK4) method provides a high degree of accuracy. It updates the solution as:

$$y_{n+1} = y_n + \frac{h}{6}(k_1 + 2k_2 + 2k_3 + k_4),$$

where:

$$k_1 = f(t_n, y_n), \quad k_2 = f\left(t_n + \frac{h}{2}, y_n + \frac{h}{2}k_1\right),$$

$$k_3 = f\left(t_n + \frac{h}{2}, y_n + \frac{h}{2}k_2\right), \quad k_4 = f(t_n + h, y_n + hk_3).$$

The adaptive version (RK45) dynamically adjusts h based on error estimates, making it more efficient for varying dynamics [?].

4.4 Implicit Backward Euler Method

The backward Euler method is a first-order implicit scheme, given by:

$$y_{n+1} = y_n + hf(t_{n+1}, y_{n+1}).$$

This method is unconditionally stable and effective for stiff systems, but requires iterative solvers to handle the implicit nature [?].

4.5 Crank-Nicolson Method

The Crank-Nicolson method combines forward and backward Euler schemes:

$$y_{n+1} = y_n + \frac{h}{2}\left[f(t_n, y_n) + f(t_{n+1}, y_{n+1})\right].$$

This second-order implicit method is stable and accurate for oscillatory systems [?].

4.6 Leapfrog Method

The leapfrog method updates positions and velocities alternately:

$$r_{n+1} = r_n + hv_{n+1/2}, \quad v_{n+3/2} = v_{n+1/2} + ha_{n+1}.$$

It is time-reversible, energy-conserving, and suitable for conservative systems, but less effective for systems with strong damping or stiffness [?].

4.7 Symplectic Integrators

Symplectic integrators, such as the velocity Verlet or implicit midpoint rule, are designed for Hamiltonian systems. For the implicit midpoint rule:

$$y_{n+1} = y_n + hf\left(\frac{t_n + t_{n+1}}{2}, \frac{y_n + y_{n+1}}{2}\right).$$

These methods preserve energy and momentum over long simulations but require implicit solvers [?].

4.8 Exponential Integrators

Exponential integrators solve linear components of ODEs analytically using:

$$y_{n+1} = e^{Ah} y_n + \int_0^h e^{A\tau} g(y_n) d\tau,$$

where A represents the linear operator. These methods are ideal for oscillatory systems or systems with stiffness [?].

4.9 Multiscale Methods

Multiscale methods address systems with multiple timescales by separating fast and slow dynamics. The heterogeneous multiscale method (HMM) is one example, where a reduced model is used for the slow dynamics, while the fast dynamics are simulated only as needed [?].

4.10 Geometric Integrators

Geometric integrators, such as discrete gradient methods, preserve invariants like energy or angular momentum. These methods are particularly useful for long-term simulations of conservative systems [?].

4.11 Methodology Selection

Considering the nonlinear coupling, oscillatory dynamics, and periodic forcing in the spring pendulum system:

- RK4 is the preferred choice for its high accuracy and efficiency in solving nonlinear systems.
- Adaptive RK45 is recommended for simulations with varying dynamics or fast transitions.
- Symplectic integrators are suitable for long-term energy conservation in undamped or weakly damped systems.

Based on these considerations:

1. The Euler method is unsuitable due to its low accuracy and conditional stability.

2. Verlet integration is effective for conservative dynamics but less ideal for velocity-dependent damping or magnetic forces.

3. The RK4 method offers high accuracy and is appropriate for the nonlinear coupled equations of motion, making it the preferred choice.

4. Implicit methods, such as backward Euler or Crank-Nicolson, are robust but computationally expensive due to the implicit nature.

5. The leapfrog method is suitable for conservative dynamics but less flexible for velocity-dependent forces.

Thus, the fourth-order Runge-Kutta method (RK4) is selected for its balance between accuracy, stability, and computational efficiency.

5 Numerical Results and Visualizations

The numerical simulation of the spring pendulum system with magnetic interaction was performed using the fourth-order adaptive Runge-Kutta method (RK45). The system's dynamics were visualized using animations, phase portraits, and a Poincaré map, as described below.

5.1 Animation of the System Dynamics

A GIF animation was created to visualize the motion of the spring pendulum over time. The animation captures:

- The oscillatory motion of the mass in the radial and angular directions.
- The periodic forcing due to the oscillating magnetic field.
- Real-time display of the system's configuration, including the spring and pendulum motion.

The animation provides an intuitive understanding of the coupled dynamics of the system, highlighting the influence of the magnetic field and nonlinear coupling. The GIF file is named `spring_pendulum.gif`.

5.2 Radial Phase Portrait

The radial phase portrait, shown in Figure 2, plots the spring length (r) versus its radial velocity ($\dot{r}$):

$$\text{Radial Phase Portrait:} \quad r \text{ vs. } \dot{r}.$$

This visualization highlights the oscillatory behavior in the radial direction, showing the cyclic nature of the spring's extension and compression.

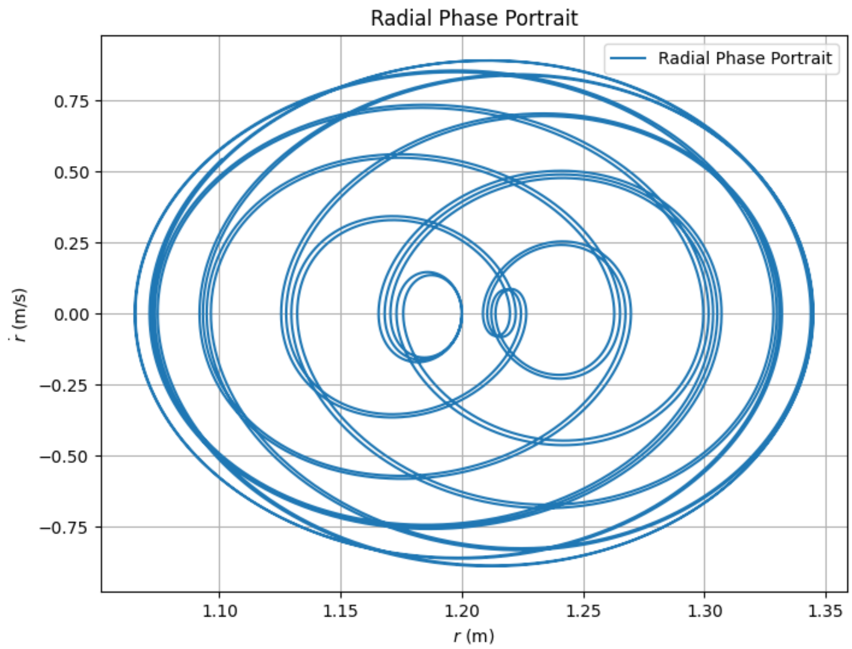

Figure 2: Radial phase portrait showing the relationship between the spring length r and its radial velocity $\dot{r}$.

5.3 Angular Phase Portrait

The angular phase portrait, shown in Figure 3, plots the angular displacement (θ) versus its angular velocity ($\dot{\theta}$):

$$\text{Angular Phase Portrait:} \quad \theta \text{ vs. } \dot{\theta}.$$

This plot captures the periodic nature of the pendulum's angular motion, including the influence of the nonlinear coupling and magnetic forcing.

5.4 Poincaré Map

The Poincaré map, shown in Figure 4, visualizes the system's periodic dynamics by sampling the angular displacement (θ) and angular velocity ($\dot{\theta}$) at discrete times corresponding to the period of the magnetic field:

$$T = \frac{2\pi}{\omega}.$$

This map provides insights into the system's stability and periodicity, showing how the dynamics evolve over successive periods of the magnetic forcing.

5.5 Discussion of Results

The numerical and visual analysis highlights several key aspects of the system:

- The radial and angular phase portraits demonstrate the cyclic nature of the spring-pendulum motion, with nonlinear effects visible in the trajectories.

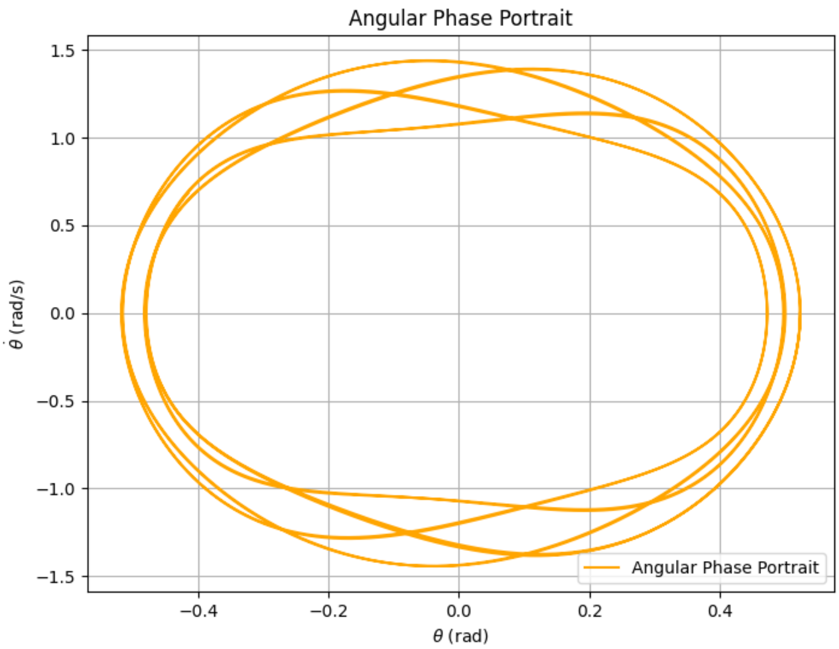

Figure 3: Angular phase portrait showing the relationship between the angular displacement θ and angular velocity $\dot{\theta}$.

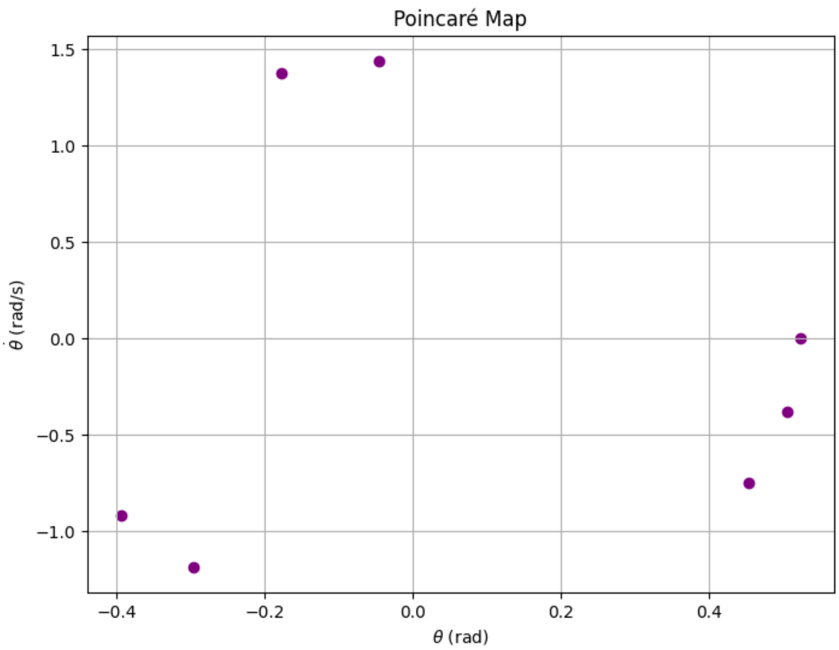

Figure 4: Poincaré map showing the angular displacement θ and angular velocity $\dot{\theta}$ sampled at intervals of the magnetic field period $T = \frac{2\pi}{\omega}$.

- The Poincaré map shows the influence of periodic magnetic forcing, revealing patterns of stability or chaos depending on the system's parameters.

- The animation provides an intuitive visualization of how the magnetic field modulates the spring and pendulum dynamics in real-time.

These visualizations collectively provide a comprehensive understanding of the spring pendulum's behavior under magnetic forcing.

6 Magnetic Interaction Modeling

This section focuses on refining the magnetic field model and incorporating enhanced magnetic forces into the spring pendulum system. These refinements allow for a more accurate representation of the ferromagnetic interaction and its impact on system dynamics.

6.1 Enhanced Magnetic Field Model

The magnetic field is extended to include spatial and temporal variations:

$$\mathbf{B}(\mathbf{r}, t) = B_0 \cos(\omega t)\hat{z} + \nabla\Phi(\mathbf{r}),$$

where $\Phi(\mathbf{r})$ can represent spatial variations, such as:

- A uniform field: $\Phi(\mathbf{r}) = 0$.
- A dipole field:
$$\mathbf{B}(\mathbf{r}) = \frac{\mu_0}{4\pi}\frac{3(\mathbf{m}\cdot\hat{r})\hat{r} - \mathbf{m}}{r^3}.$$

6.2 Nonlinear Magnetic Force

The magnetic force acting on the mass is expressed as:

$$\mathbf{F}_m = \nabla(\mu \cdot \mathbf{B}) = \mu(\nabla \cdot \mathbf{B}) + (\mu \cdot \nabla)\mathbf{B}.$$

Nonlinear effects such as magnetic hysteresis and saturation can be included:

- **Hysteresis:** The magnetic moment μ depends on the history of $B(t)$.
- **Saturation:** The magnetic moment asymptotically approaches a maximum value:
$$\mu(B) = \frac{\mu_{\max} B}{B + B_s}.$$

6.3 Updated Equations of Motion

The equations of motion are modified to include the enhanced magnetic force terms:

$$\ddot{r} = r\dot{\theta}^2 - \frac{k}{m}(r - l_0) + g\cos\theta + \frac{\mu}{m}\frac{\partial B}{\partial r},$$

$$\ddot{\theta} = -\frac{2\dot{r}\dot{\theta}}{r} - \frac{g}{r}\sin\theta + \frac{\mu}{mr}\frac{\partial B}{\partial \theta}.$$

6.4 Numerical Implementation

The numerical solver is updated to include:

- Computation of the refined magnetic field $\mathbf{B}(\mathbf{r}, t)$.
- Inclusion of nonlinear magnetic forces $\mathbf{F}_m$ in the equations of motion.

5. Analysis and Visualization

To assess the impact of the refined magnetic modeling, the following visualizations are generated:

- **Phase Portraits:** Compare the radial and angular phase space trajectories.
- **Poincaré Maps:** Highlight differences in periodicity and stability.
- **Time-Series Plots:** Illustrate changes in the radial and angular motion over time.

6.5 Discussion

The refined magnetic interaction modeling provides a more realistic representation of the ferromagnetic system. The added complexity introduces new dynamics, including stronger nonlinear coupling and potential chaotic behavior.

7 Spring Pendulum with Magnetic Interaction: Numerical Analysis

This document outlines the numerical simulation of a spring pendulum system with enhanced magnetic interaction. The system's dynamics are analyzed using numerical methods, phase portraits, Poincaré maps, and animations.

8 Numerical Techniques

The equations of motion for the spring pendulum system are solved using the RK45 method, which adapts the time step to balance accuracy and efficiency. The Python implementation includes enhancements for capturing nonlinear effects, especially in the presence of an oscillating magnetic field.

9 Enhanced Magnetics

The magnetic field model was extended to include dynamic behavior based on saturation effects. The interaction between the magnetic field and the ferromagnetic mass was modeled as:

$$\mathbf{F}_m = \nabla(\mu \cdot \mathbf{B}),$$

where μ is the magnetic moment, which varies dynamically according to:

$$\mu(B) = \frac{\mu_{\max} B}{B + B_s}.$$

9.1 Radial Phase Portrait

The radial phase portrait, shown in Figure 5, plots the spring length r versus its radial velocity $\dot{r}$. It illustrates the periodic oscillations in the radial direction, highlighting nonlinear coupling introduced by the magnetic interaction.

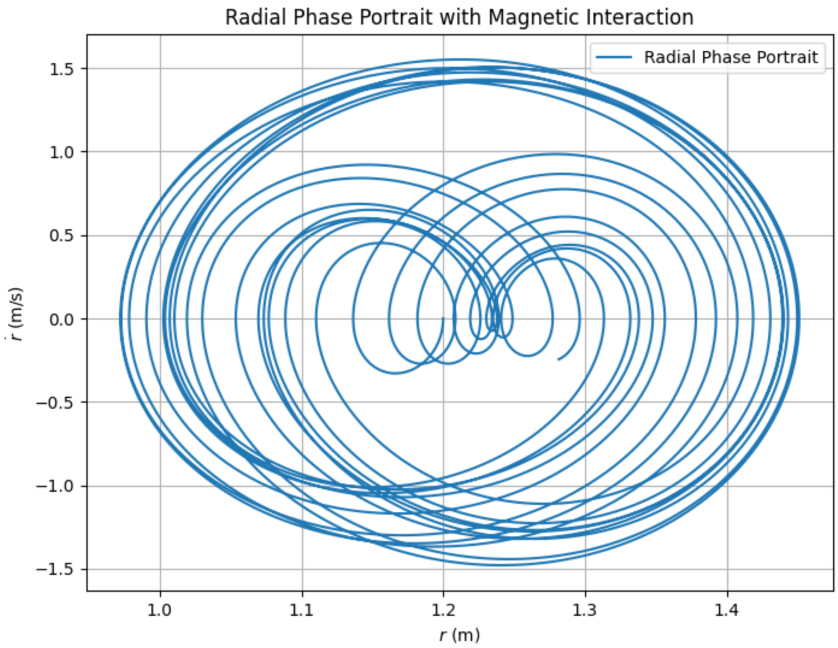

Figure 5: Radial phase portrait: r vs. $\dot{r}$. The plot shows the effect of the enhanced magnetic interaction on the radial motion.

9.2 Angular Phase Portrait

The angular phase portrait, shown in Figure 6, plots the angular displacement θ versus its angular velocity $\dot{\theta}$. It reveals the impact of the oscillating magnetic field on the angular motion.

9.3 Poincaré Map

The Poincaré map, shown in Figure 7, samples the angular displacement θ and angular velocity $\dot{\theta}$ at intervals corresponding to the period of the magnetic field:

$$T = \frac{2\pi}{\omega}.$$

The map captures periodicity and chaotic behavior in the system's dynamics.

9.4 Animation

An animation of the system's motion was created to visualize the dynamic behavior. The animation illustrates:

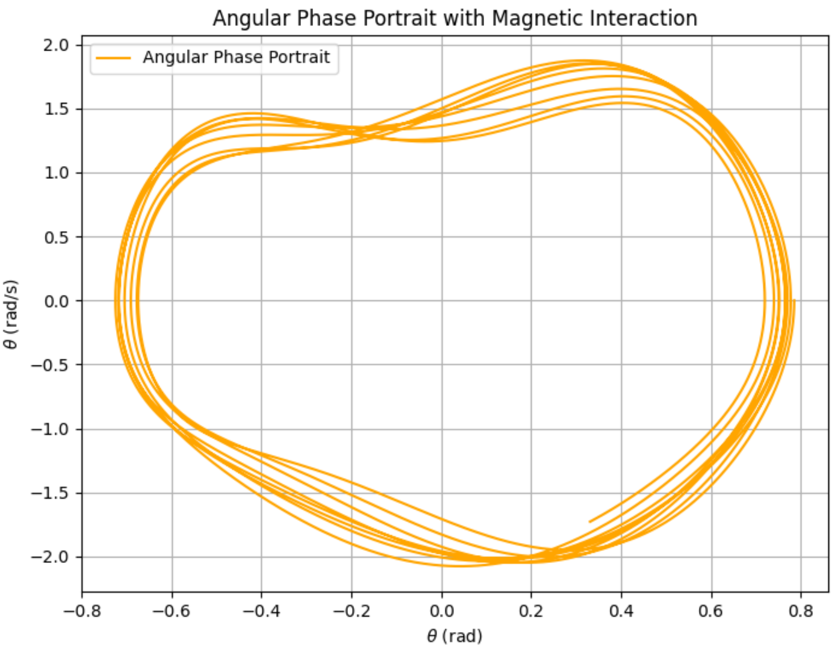

Figure 6: Angular phase portrait: θ vs. $\dot{\theta}$. Nonlinear effects from the magnetic forcing are evident.

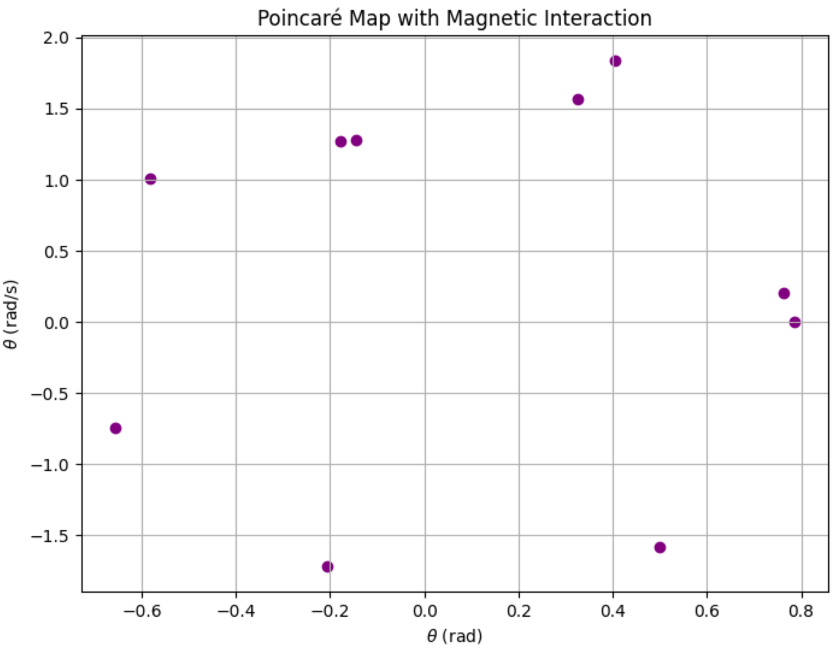

Figure 7: Poincaré map: θ vs. $\dot{\theta}$ sampled at the period of the magnetic field.

- Coupled radial and angular motion.
- The influence of the magnetic field on the pendulum's dynamics.
- Real-time visualization of the spring's oscillations and pendulum's angular motion.

The animation is saved as a GIF file, named `spring_pendulum_magnetic.gif`.

10 Discussion

The enhanced magnetic interaction introduces complex nonlinear effects into the system, resulting in more intricate dynamics. Visualizations, including phase portraits and Poincaré maps, reveal the interplay between periodic forcing and nonlinear coupling. The numerical simulation demonstrates the system's sensitivity to parameter changes, offering insights into chaotic and quasi-periodic behavior.

11 Conclusion

The refined magnetic model adds depth to the analysis of the spring pendulum system, capturing nonlinear effects and enhancing the realism of the simulation. Future work can explore the system's behavior under varying damping and additional external forces.